HHS Public Access

Author manuscript

J Neurochem. Author manuscript; available in PMC 2016 November 01.

Published in final edited form as:

J Neurochem. 2015 November ; 135(4): 695–704. doi:10.1111/jnc.13286.

Comparison of Dopamine Kinetics in the Larval *Drosophila* Ventral Nerve Cord and Protocerebrum with Improved Optogenetic Stimulation

Eve Privman and **B. Jill Venton**

Department of Chemistry, Neuroscience Graduate Program, and Medical Scientist Training Program, University of Virginia

Abstract

Dopamine release and uptake have been studied in the *Drosophila* larval ventral nerve cord (VNC) using optogenetics to stimulate endogenous release. However, other areas of the central nervous system remain uncharacterized. Here, we compare dopamine release in the VNC and protocerebrum of larval *Drosophila.* Stimulations were performed with CsChrimson, a new, improved, red light-activated channelrhodopsin. In both regions, dopamine release was observed after only a single, 4 ms duration light pulse. Michaelis-Menten modeling was used to understand release and uptake parameters for dopamine. The amount of dopamine released ($[DA]_p$) on the first stimulation pulse is higher than the average $[DA]_p$ released from subsequent pulses. The initial and average amount of dopamine released per stimulation pulse is smaller in the protocerebrum than in the VNC. The average V_{max} of 0.08 μM/s in the protocerebrum was significantly higher than the V_{max} of 0.05 μM/s VNC. The average K_m of 0.11 μM in the protocerebrum was not significantly different from the K_m of 0.10 μM in the VNC. When the competitive dopamine transporter (DAT) inhibitor nisoxetine was applied, the K_m increased significantly in both regions while V_{max} stayed the same. This work demonstrates regional differences in dopamine release and uptake kinetics, indicating important variation in the amount of dopamine available for neurotransmission and neuromodulation.

Graphical Abstract

Laboratory of Origin: B. Jill Venton, PO Box 400319, Charlottesville, VA 22904, jventon@virginia.edu, p: (434) 243-2132, f: (434) 924-3710

Conflicts of interest: none

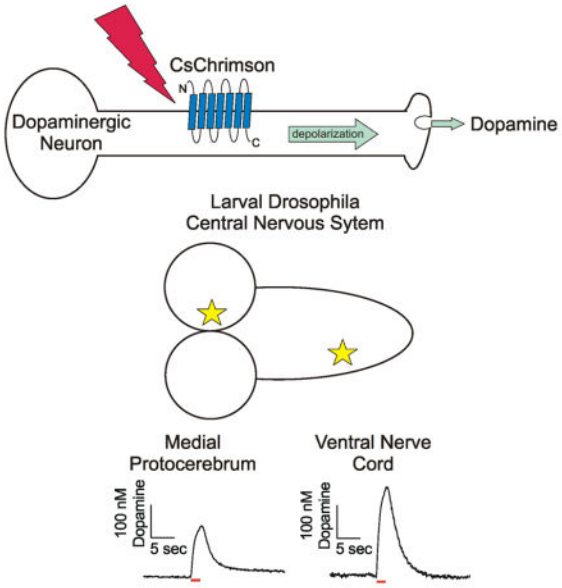

Keywords

Drosophila; dopamine; optogenetics; FSCV; kinetic modeling; voltammetry

Introduction

There are a vast array of genetic tools available to study *Drosophila melanogaster*, making it a powerful and convenient model organism (Martin and Krantz, 2014). The basic mechanisms of neurotransmission are evolutionarily conserved, allowing for the study of human neurological diseases in *Drosophila* (Pandey and Nichols, 2011). There are approximately 90 dopaminergic neurons in the larval *Drosophila* central nervous system, organized into clusters in the protocerebrum, subesophageal zone, and the ventral nerve cord (VNC) (Selcho et al., 2009). Each region mediates specific physiological responses and behaviors. Dopaminergic neurons in the VNC function in motor behaviors such as grooming and copulation (Yellman et al., 1997; Crickmore and Vosshall, 2013), dopaminergic neurons in the protocerebrum control olfactory learning and memory (Selcho et al., 2009), and dopaminergic neurons in the subesophageal ganglion trigger proboscis extension as part of the primary taste relay (Marella et al., 2012). Direct measurements of endogenous dopamine have only been made in the larval VNC (Borue et al., 2009; Vickrey et al., 2009; Xiao et al., 2014).

In *Drosophila* larvae, Channelrhodopsin-2 (ChR2) is a cation channel that has been used to evoke endogenous neurotransmitter release, which is measured using an implanted microelectrode (Vickrey et al., 2009, 2013; Borue et al., 2010; Vickrey and Venton, 2011). Optogenetic stimulation can be used to excite subpopulations of neurons by targeting specific neurotransmitter synthesis pathways using the Gal4/UAS system (Duffy, 2002; Nagel et al., 2003). ChR2 responds to blue light, which does not penetrate deeply into tissue and can cause an aberrant signal near the switching potential in electrochemical recordings

(see Supplemental Figure 1) (Vickrey et al., 2009; Bass et al., 2013; Xiao et al., 2014). Recently, there has been interest in shifting from blue to red light activated channelrhodopsins (Nagel et al., 2003; Lin et al., 2013; Klapoetke et al., 2014). Red light penetrates deeper and is less visible to flies, making it more useful in behavioral experiments. Klapoetke *et al* (2014) characterized the cation channel CsChrimson in *Drosophila*, controlling neuronal activation using short, low-intensity, red light stimulations.

Dopamine is cleared from the extracellular space by uptake through *Drosophila* dopamine transporters (dDAT) (Pörzgen et al., 2001). dDAT regulation of extracellular dopamine has been studied by exogenously applying dopamine (Makos et al., 2009, 2010; Berglund et al., 2013) and then modeling the clearance using Michaelis-Menten kinetics (Sabeti et al., 2002; Vickrey et al., 2013). Alternatively, stimulated endogenous dopamine release can be modeled to extract Michaelis-Menten values. Studying endogenous dopamine is advantageous because physiological amounts are measured and the dopamine released per stimulation pulse can be modeled. In mammals, dopamine release and clearance kinetics vary by brain region due to differential terminal density and DAT expression (Wu et al., 2001) and we hypothesize that distinct *Drosophila* neuropil will also have differences in release and uptake.

Here, we compare dopamine release in the *Drosophila* larval VNC and protocerebrum. The amount of dopamine released was high with CsChrimson-mediated stimulations and it could be measured after a single, 4 ms pulse of red light. Stimulated dopamine release was larger in the VNC than the protocerebrum, and the regions exhibited different uptake kinetics.

Materials and Methods

Chemicals

All chemicals were purchased from Sigma-Aldrich (St. Louis, MO) and all solutions were made with Milli-Q water (Millipore, Billerica, MA). Dissections, recordings, and calibrations were performed in a simple physiological solution (131.3 mM NaCl, 3.0 mM KCl, 10 mM NaH_2PO_4 monohydrate, 1.2 mM $MgCl_2$ hexahydrate, 2.0 mM Na_2SO_4 anhydrous, 1.2 $CaCl_2$ dihydrate, 11.1 mM glucose, 5.3 mM trehalose, pH = 7.4). A concentrated stock solution of nisoxetine was made in buffer and added to the sample for a final concentration of 20 μM.

Electrochemical Measurements

Carbon fiber microelectrodes were fabricated from T-650 carbon fibers (a gift of Cytec Engineering Materials, West Patterson, NJ) as previously described (Jacobs et al., 2011). Electrodes were calibrated *in vitro* using a flow cell to alternatively apply buffer and buffer containing 1 μM dopamine to determine the unique response to 1 μM dopamine for each electrode. The amount of dopamine measured *in vivo* is then calculated using this calibration factor, since the measured peak oxidation current for dopamine increases linearly with dopamine concentration within the physiological range. Fast-scan cyclic voltammetry was performed using a ChemClamp potentiostat with a n=0.01 headstage (Dagan, Minneapolis, MN), PCI 6711 and 6052 computer interface cards (National Instruments, Austin, TX), and

a home built break-out box. The TarHeel CV software (a gift of Mark Wightman, University of North Carolina) was used to collect and background subtract the data. Every 100 ms the electrode was scanned from −0.4 to 1.3 V at 400 V/s.

Tissue Preparation

Virgin females with UAS-CsChrimson (a chimera of CsChR and Chrimson; a gift of Vivek Jayaraman) inserted in attp18 (Klapoetke et al., 2014) were crossed with TH-GAL4 (a gift of Jay Hirsh). Resulting heterozygous larvae were shielded from light and raised on standard cornmeal food mixed 250:1 with 100 mM all-trans-retinal (Sigma-Aldrich, St. Louis, MO). A small amount of moistened Red Star yeast (Red Star, Wilwaukii, WI) was placed on top of the food to promote egg laying. The central nervous system of third instar wandering larvae of either sex were dissected out in buffer. Isolated VNCs were prepared and recorded from as previously described (Borue et al., 2009). For the protocerebrum recordings, the CNS was placed on an uncoated Petri dish dorsal side down. A small slice of the lateral optic lobe was removed using the tip of a 22-gauge hypodermic needle. The electrode was implanted from the lateral edge of the tissue into the dorsal medial protocerebrum. The electrode was allowed to equilibrate in the tissue for 10 minutes prior to data collection. A baseline recording was taken for 10 seconds prior to stimulation.

Stimulated Neurotransmitter Release

Red-orange light from a 617 nm fiber-coupled high-power LED with a 200 μm core optical cable (ThorLabs, Newton, NJ) was used to stimulate the CsChrimson ion channel. A commercial power meter (Coherent Incorporation, Santa Clara, CA) estimated the output power at 0.75 mW. The fiber was centered pointing at the brain region being monitored by the recording electrode and positioned 75–100 um from the sample using a micromanipulator. The light was modulated with Transistor-Transistor Logic (TTL) inputs to a T-cube LED controller (ThorLabs, Newton, NJ), which was connected to the breakout box. TTL input was driven by electrical pulses controlled by the TarHeel CV software, which was used to control frequency, pulse width, and number of pulses.

Statistics and Data Analysis

Data are presented as mean +/− standard error of the mean (SEM) displayed as error bars. GraphPad Prism 6 (GraphPad Software Inc, La Jolla, CA) was used to perform all statistics, including one-way and two-way ANOVA with Bonferonni post-hoc test. Stimulated changes in the extracellular concentration of dopamine were modeled as a balance between discontinuous release and continuous uptake (Wu et al., 2001). A nonlinear regression with a simplex minimization algorithm was used to fit the curves (Garris and Wightman, 1995). The modeling software was stopped when the iteration number continued increasing without a change in the three floated parameters. The goodness of the fit was described using the square regression coefficient (R^2). The R^2 fitting values for the two-second stimulations in the VNC were 0.94+/−0.01 (n=19) and in the protocerebrum were 0.91+/−0.02 (n=8). The average values of kinetic parameters were obtained by fitting data from 2 second long stimulations with 4 ms pulses at 60 Hz.

Results

Dopamine release was stimulated by red light (617 nm) from dopaminergic neurons in th-Gal4;UAS-CsChrimson larvae. Changes in dopamine concentration were measured with fast-scan cyclic voltammetry. For the VNC measurements, the 7 μm diameter carbon-fiber microelectrode was positioned in the neuropil of the isolated VNC (Fig 1A). A false color plot shows all the data collected with the background-subtracted current plotted in false color, applied potential on the y-axis, and time on the x-axis. Figure 1B shows an example of a 2 s continuous stimulation in the VNC, where dopamine oxidation (green) and reduction (dark blue) were observed around the expected potentials of 0.6 V and −0.2 V, respectively (Garris and Wightman, 1995). The cyclic voltammograms, a plot of current vs voltage, provide an electrochemical fingerprint to help identity dopamine (Fig 1C). The shape and location of the oxidation and reduction peaks in the cyclic voltammogram are different than other fly neurotransmitters, such as serotonin and octopamine. In addition, the specific targeting of the dopaminergic synthetic pathway with the th-GAL4 driver helps provide confident identification of the released electroactive compound as dopamine. Repeated stimulations in the presence of the serotonin synthesis blocker PCPA did not significantly decrease the signal as it does for serotonin release (Borue et al., 2009), indicating that secondary serotonin release does not contribute significantly to the measured current (Supplemental Fig S2). The concentration of dopamine in the extracellular space of the VNC increased while the light was on, and then quickly returned towards baseline when the light was turned off (Fig 1D). This indicates that the dopamine is released as a consequence of the light stimulation and no downstream product due to dopamine release is detected that would appear after the light is turned off.

Dopamine release and uptake were also monitored in a novel region of the *Drosophila* central nervous system: the protocerebrum. The carbon-fiber microelectrode was inserted into the medial protocerebrum through a lateral cut in the tissue (Fig 2A). Similarly to the VNC, extracellular dopamine concentration was evoked by 2 s continuous light and measured over time (Fig 2B and D). The identity of dopamine is confirmed by the cyclic voltammogram, which has oxidation and reduction peaks occurring at the same potentials as in the VNC (Fig 2C). Note that the y-scale bar in Figure 1D is larger than in 2D, because the measured dopamine release was larger in the VNC than in the protocerebrum.

In previous studies using blue light to stimulate ChR2 mediated release, an error was observed at the switching potential due to the photoelectric effect (Vickrey et al., 2009; Bass et al., 2013). With red light that error is eliminated (Supplemental Fig S1), because the light is not of sufficient energy to interfere with the electrode. There is a slight decrease in current centered around 0 V in the cyclic voltammograms (Fig 1C, 2C), but this peak is likely due to changes in pH or extracellular calcium concentrations due to the rapid, simultaneous depolarization of many dopaminergic neurons (Takmakov et al., 2010). The peak is not at the same potential as dopamine oxidation (0.6 V) or reduction (−0.2 V) and therefore does not interfere with dopamine detection.

In order to show that CsChrimson can be used to mimic different firing patterns, short pulses of red light were used to elicit dopamine release from the VNC and protocerebrum.

Increasing concentrations of dopamine were detected with increasing number of pulses (Fig 3A). As the number of 4 ms light pulses increased from 1 to 120 at a frequency of 60 Hz, there was an increase in peak extracellular dopamine concentration (Fig 3B). However, the increase was not linear, indicating more dopamine was released for the first few pulses. A two-way ANOVA indicates a main effect of pulse number ($p<0.0001$, n=5–7) and brain region ($p<0.0001$, n=5–7), and no interaction. The protocerebrum releases less dopamine than the VNC. The data for each animal were then normalized to 2 second continuous stimulations to account for differences in release between animals (Fig 3C). The amount of dopamine release by pulsed stimulations was always less than or equal to the 2 s continuous stimulation. The normalized data reveal that the shape of the curves for the VNC and protocerbrum are similar. A two-way ANOVA indicates a main effect of pulse number ($p<0.0001$, n=5–7), but no effect due to brain region and no interaction.

The effect of varying red light pulse frequency was tested in both regions, using frequencies of 10–120 Hz for 2 seconds total stimulus duration (Fig 4A, each pulse is 4 ms). For example there were 20 pulses at 10 Hz and 200 pulses at 100 Hz. The peak oxidation current for dopamine was normalized to a two second continuous stimulation for each animal. Increasing the frequency of the light pulses (Fig 4B) increased the extracellular dopamine concentration in the VNC (one-way ANOVA, $p<0.0001$, n=7–9) and in the protocerebrum (one-way ANOVA, $p=0.0007$, n=5–7). The pulsed stimulation is no longer significantly different from the continuous stimulation (100%) above 80 Hz in the VNC and above 60 Hz in the protocerebrum ($p>0.05$, Bonferroni post-hoc t-tests). A two-way ANOVA indicates that there is a main effect of both frequency ($p<0.0001$) and brain region ($p<0.0001$), and no interaction. The normalized extracellular dopamine is significantly higher in the VNC than in the protocerebrum at 10 and 20 Hz ($p<0.01$, Bonferroni post-hoc tests).

Using the 60 Hz, 120 pulse pulsed stimulation data, we modeled the release and uptake of dopamine in the VNC (Fig 5A, average $R^2=0.94$) and protocerebrum (Fig 5B, average $R^2=0.91$). The model (in black) is a nonlinear regression with a simplex minimization algorithm (Garris and Wightman, 1995), which regards the extracellular concentration of dopamine as a balance between the pulsed release of dopamine and its continuous uptake. The average dopamine released per pulse is assumed to be the same for all pulses. $[DA]_p$, V_{max}, and K_m are summarized in Table 1. The dopamine released per pulse was significantly lower in the protocerebrum (n=8) than in the VNC (n=19) (unpaired t-test, $p=0.0062$), while the V_{max} was significantly higher in the protocerebrum than in the VNC ($p=0.0447$, unpaired t-test). The K_m was not significantly different between the two regions ($p>0.05$, unpaired t-test).

Because the pulse number data from Figure 3 indicated the first pulses release more dopamine than subsequent pulses, one pulse stimulations were also modeled to gain a better understanding of the initial $[DA]_p$. The one pulse data are noisier, but the fits were still acceptable in the VNC (Fig 5C, average $R^2=0.88$) and protocerebrum (Fig 5D, average $R^2=0.84$). The resulting data, summarized in Table 1, show that $[DA]_p$ values were significantly larger with one pulse stimulations than the average $[DA]_p$ with 120 pulses in both the VNC ($p=0.0195$, unpaired t-test) and protocerebrum ($p=0.0322$, unpaired t-test). For both regions, the initial $[DA]_p$ was about 30 times the average for the 2 second pulse

train, indicating that $[DA]_p$ drops off dramatically with subsequent pulses. Supplemental Figure 3 shows that for the data in both regions $[DA]_p$ drops off exponentially with pulse number, plateauing at 0.76 nM in the VNC and 0.41 nM in the protocerebrum. As expected, the number of pulses did not affect uptake values and K_m and V_{max} did not significantly differ in 1 pulse versus the longer stimulation data ($p>0.05$, unpaired t-tests).

Finally, the effect of the dDAT blocker nisoxetine was measured in the VNC and protocerebrum. Nisoxetine was used at a concentration previously shown to impair the flux of dopamine through dDAT (Pörzgen et al., 2001). In both regions, the clearance of stimulated extracellular dopamine was slowed 15 minutes after 20 μM nisoxetine application (Fig 6A, B). Two second long, 10 and 60 Hz stimulations were applied and the predrug and nisoxetine data were modeled as before. There was a significant main effect of drug on the apparent K_m (two-way ANOVA; $p=0.0310$, n=5–8), but not on V_{max} (two-way ANOVA; $p>0.05$, n=5–8) (Fig 6C). An increase in K_m and no change in V_{max} is consistent with nisoxetine acting as a competitive antagonist at dDAT.

Discussion

We measured dopamine release stimulated by CsChrimson activation of dopamine neurons in two distinct regions of the larval *Drosophila* central nervous system: the protocerebrum and VNC. Released dopamine could be measured after a single pulse of light using CsChrimson stimulation. The initial and average $[DA]_p$ is smaller in the protocerebrum than the VNC. The average K_m for uptake was the same in both regions, however the V_{max} was higher in the protocerebrum than in the VNC. Thus, although there is a lower amount of dopamine released in the protocerebrum after similar stimulation, there is a higher dopamine transporter density for clearance. The dDAT blocker nisoxetine acted as a competitive inhibitor, significantly increasing the K_m in both regions. Dopamine release and regulation by dDAT vary in different *Drosophila* neuropil, which leads to different amounts of dopamine available for signaling.

Dopamine Release in the VNC and Protocerebrum

Upon red light stimulation, CsChrimson expressed in the cell membranes of targeted cells will open, allowing an inward flow of cations that depolarizes the cell. Previous electrophysiological studies of CsChrimson have shown that repeated 5 ms pulsed stimulations at frequencies greater than 10 Hz do not reliably produce an action potential every time (Klapoetke et al., 2014). However, with ChR2 it has been noted that increases in neurotransmitter release occur at higher stimulation frequencies than would be expected from the channel photocycle kinetics (Bamann et al., 2008; Xiao et al., 2014). CsChrimson mediated release was frequency dependent up to 60 Hz in both regions, which is consistent with previous work in flies and mammals (Wightman and Zimmerman, 1990; Xiao et al., 2014). CsChrimson kinetics were not limiting to the present study, likely because release comes from a population of neurons, which release more dopamine with higher frequencies even if not every individual neuron produces an action potential with every stimulation pulse.

CsChrimson facilitated the measurement of stimulations with as little as a single pulse, in comparison to previous studies with ChR2, where at least 10 stimulation pulses were needed (Xiao et al., 2014). In mammals, dopaminergic cells are known to fire spontaneously in average bursts of 3–4 spikes at approximately 14 Hz (Grace and Bunney, 1984), so the ability to study short pulse trains is advantageous for mimicking neuronal burst firing. Shorter stimulations also avoid the effects of uptake (Garris et al., 1994). The amount of dopamine released by small stimulations is much higher than expected if every pulse were to release the same amount of dopamine. For example, 1 pulse produced 20% of the signal elicited by 120 pulses in the VNC. The $[DA]_p$ for the initial stimulation is 30 times the average for a longer pulse train. Thus, the initial pulses in *Drosophila* produce more $[DA]_p$ than later stimulations in the train. This could be due to depletion of the dopamine pools with longer stimulation times or autoreceptor regulation (Vickrey and Venton, 2011). Earlier research in mammals found that 4 pulses elicited 4 times the concentration of a single pulse in the presence of a dopamine uptake inhibitor, so $[DA]_p$ was assumed to be the same for each pulse (Garris et al., 1994). However, recent work in mammals has also begun to recognize the heterogeneity in the amount of dopamine released during a long pulsed stimulation (Taylor et al., 2015). Future models for longer pulse trains could model the changes in $[DA]_p$ and account for the exponential decay in release. The uptake kinetics for single-pulse and longer trains were not different, so longer pulse trains can be used to examine uptake.

Dopamine released per pulse was significantly lower in the protocerebrum than in the VNC. This difference could be due to a lower density of dopaminergic synapses in the medial protocerebrum than in the compact, highly innervated neuropil of the VNC (Selcho et al., 2009). In the medial protocerebrum there are projections from approximately 20 dopaminergic cells in three clusters (DM, DL1, and DL2) per lobe (Pörzgen et al., 2001). In the VNC, there are approximately 22 neurons that send projections to the densely innervated, sheathed neuropil. Dopaminergic neurons acting in a neuromodulatory capacity, such as those in the protocerebrum, would have diffuse projections rather than forming direct synapses (Selcho et al., 2009). The lower dopamine per pulse measured in the protocerebrum could therefore be due to fewer dopaminergic synapses or less releasable dopamine per synapse.

Uptake Kinetics in the VNC and Protocerebrum

The uptake kinetics of dopamine were obtained from the modeled pulsed stimulation data in the VNC and protocerebrum. Uptake of dopamine through dDAT is assumed to follow Michaelis-Menten kinetics. V_{max} is a function of the density of the transporters and K_m is a measure of the affinity of the transporter for dopamine. As expected, K_m and V_{max} were unaffected by the number of stimulation pulses. K_m was not significantly different in the VNC and protocerebrum, which indicates that dDAT has a consistent affinity for dopamine. V_{max} was significantly higher in the protocerebrum than in the VNC. More tightly regulated neuromodulatory dopaminergic projections in the protocerebrum (Selcho et al., 2009) may account for the higher V_{max} due to more dense expression of dDAT for uptake. There may be N-terminal serine phosphorylation of DAT as there is in the rat (Foster et al., 2002) that changes the transport speed or surface expression of DAT in different regions of the

Drosophila brain. Different splice variants of dopamine receptors may also be interacting with and stabilizing DAT differently in the presynaptic membrane of subsets of dopaminergic cells (Sullivan et al., 2013). Good staining methods for dDAT have not been optimized, but future work can look into the expression levels of dDAT in different regions of the *Drosophila* brain.

The consequence of the varying uptake and release per pulse is that different amounts of dopamine are available for signaling in the protoecerbrum and the VNC. Lower extracellular concentrations of dopamine are present in the medial protocerebrum, reflected in its smaller release and faster uptake. The medial protocerebrum is active in sensory learning and memory, which may not require as much dopamine for activation due to receptor sensitivity in this region. Sensory learning and memory may also be less important in this wandering stage of larvae. On the other hand dopamine neurons in the VNC are primarily involved in motor regulation. Locomotion may require more dopamine signaling and may be more active in this stage of larvae.

Here, the average K_m in the VNC is 0.10 ± 0.01 μM, which is the same order of magnitude as previous work using Channelrhodopsin-2 to stimulate release (0.45 ± 0.13 μM). However, these values are an order of magnitude lower than the previous work using dDAT transfected into MDCK cells (4.8 ± 0.4 μM) and exogenously applied dopamine in the VNC (1.3 ± 0.6 μM) (Pörzgen et al., 2001; Vickrey et al., 2013). The modeling of pulsed stimulations is more accurate, because it relies on physiological amounts of endogenous dopamine. The *Drosophila* VNC values for K_m are similar to literature values for rat DAT in the caudate putamen and nucleus accumbens (0.2 μM) (Jones et al., 1995). The V_{max} measured with CsChrimson (0.05 ± 0.01 μM/s) is also similar to that measured previously with ChR2 (0.12 ± 0.03 μM/s).

Effect of Transport Blockade in the VNC and Protocerebrum

Nisoxetine slowed clearance of stimulated extracellular dopamine in both the VNC and protocerebrum. The K_m significantly increased with nisoxetine treatment, while the V_{max} did not change. An increase in only K_m indicates that nisoxetine is acting as a competitive inhibitor at dDAT, similar to previous results from expressing dDAT in *Xenopus* oocytes (Pörzgen et al., 2001). Nisoxetine is typically used as a competitive inhibitor of the human norepinephrine transporter (hNET) (Cheetham et al., 1996), and dDAT is thought to be an evolutionary precursor to hNET (Pörzgen et al., 2001). Norepinephrine has not been found in the *Drosophila*, which instead use octopamine for neurotransmission. Octopamine has a very different cyclic voltammagram from dopamine (Denno et al., 2014). The dDAT has a higher maximal uptake velocity for dopamine than other biogenic amines, and nisoxetine is three orders of magnitude more specific for dDAT than for the serotonin transporter, the only other known transporter for amine clearance in *Drosophila* (Pörzgen et al., 2001). Therefore, the uptake inhibitor nisoxetine slowed dopamine clearance by acting as a competitive inhibitor of dDAT, affecting extracellular dopamine concentration in the expected manner in both regions of the larval CNS.

Advantages of CsChrimson Stimulation

This work demonstrates that red light stimulated CsChrimson can be used to study the release and uptake of dopamine in *Drosophila*. Traditionally, Channelrhodopsin-2 has been used for optical stimulation of neurons, but CsChrimson has several advantages over ChR2. CsChrimson is stimulated by red light instead of blue light. Blue light does not penetrate deeply into tissue due to scattering and absorption by endogenous chromophores (Lin et al., 2013). Additionally, shining blue light on the carbon-fiber microelectrode surface causes a change in surface properties, resulting in an error that been documented in both mammals (Bass et al., 2013) and flies (Vickrey et al., 2009). Red light is lower in energy and does not affect the electrode surface. CsChrimson should facilitate future work studying tyramine and octopamine, which have oxidation potentials at the switching potential (Cooper and Venton, 2009). An additional benefit of these flies is that they are heterozygous crosses between UAS-CsChrimson and th-Gal4 flies. This single cross is much easier and more stable than homozygous lines. The dopamine released per pulse, V_{max}, and K_m are all the same order of magnitude when using CsChrimson or Channelrhodopsin-2 to stimulate dopamine release from the VNC (Xiao et al., 2014). Differences in the release and uptake can be accounted for by the unique properties of the channels: light penetration, membrane expression of the channel, and photocurrent size (Klapoetke et al., 2014). Stimulations with CsChrimson can be effectively and conveniently used to characterize the different kinetics of dopamine release and uptake in *Drosophila* neuropil.

Conclusions

We measured CsChrimson stimulated dopamine release in VNC and protocerebrum of the larval *Drosophila* central nervous system. Dopamine was measured after a single pulse of light using CsChrimson stimulation, an improvement over previous studies using Channelrhodopsin-2 (Vickrey et al., 2009; Xiao et al., 2014). There is a lower amount of dopamine released in the protocerebrum than in the VNC, and there is a higher maximum rate of clearance in the protocerebrum. The dDAT blocker nisoxetine acts as a competitive inhibitor, decreasing transporter affinity in both regions. Dopamine release and regulation differ in different *Drosophila* neuropil, which leads to different amounts of extracellular dopamine available for neurotransmission and neuromodulation.

Supplementary Material

Refer to Web version on PubMed Central for supplementary material.

Acknowledgments

We thank Paul Garris and Mark Wightman for providing software and Vivek Jayaraman, Sung-Soo Kim, and Jay Hirsh for providing fly strains. This work was funded by the NIH (MH085159). The authors declare no competing financial interests. EP collected the data and EP and BJV both designed experiments, interpreted data, and wrote the article.

Abbreviations

ChR2 Channelrhodopsin-2

dDAT	*Drosophila* dopamine transporter
hNET	human norepinephrine transporter
PCPA	para-chlorophenylalanine
SEM	standard error of the mean
TTL	Transistor-Transistor Logic
VNC	Ventral Nerve cord

References

Bamann C, Kirsch T, Nagel G, Bamberg E. Spectral characteristics of the photocycle of channelrhodopsin-2 and its implication for channel function. J Mol Biol. 2008; 375:686–694. [PubMed: 18037436]

Bass CE, Grinevich VP, Kulikova AD, Bonin KD, Budygin EA. Terminal effects of optogenetic stimulation on dopamine dynamics in rat striatum. J Neurosci Methods. 2013; 214:149–155. [PubMed: 23391758]

Berglund EC, Makos MA, Keighron JD, Phan N, Heien ML, Ewing AG. Oral administration of methylphenidate blocks the effect of cocaine on uptake at the Drosophila dopamine transporter. ACS Chem Neurosci. 2013; 4:566–574. [PubMed: 23402315]

Borue X, Condron B, Venton BJ. Both synthesis and reuptake are critical for replenishing the releasable serotonin pool in Drosophila. J Neurochem. 2010; 113:188–199. [PubMed: 20070864]

Borue X, Cooper S, Hirsh J, Condron B, Venton BJ. Quantitative evaluation of serotonin release and clearance in Drosophila. J Neurosci Methods. 2009; 179:300–308. [PubMed: 19428541]

Cheetham SC, Viggers JA, Butler SA, Prow MR, Heal DJ. [3H]nisoxetine--a radioligand for noradrenaline reuptake sites: correlation with inhibition of [3H]noradrenaline uptake and effect of DSP-4 lesioning and antidepressant treatments. Neuropharmacology. 1996; 35:63–70. [PubMed: 8684598]

Cooper SE, Venton BJ. Fast-scan cyclic voltammetry for the detection of tyramine and octopamine. Anal Bioanal Chem. 2009; 394:329–336. [PubMed: 19189084]

Crickmore MA, Vosshall LB. Opposing dopaminergic and GABAergic neurons control the duration and persistence of copulation in Drosophila. Cell. 2013; 155:881–893. [PubMed: 24209625]

Denno ME, Privman E, Venton BJ. Analysis of Neurotransmitter Tissue Content of Drosophila melanogaster in Different Life Stages. ACS Chem Neurosci. 2014

Duffy JB. GAL4 system in Drosophila: a fly geneticist's Swiss army knife. Genesis. 2002; 34:1–15. [PubMed: 12324939]

Foster JD, Pananusorn B, Vaughan Ra. Dopamine transporters are phosphorylated on N-terminal serines in rat striatum. J Biol Chem. 2002; 277:25178–25186. [PubMed: 11994276]

Garris PA, Ciolkowski EL, Pastore P, Wightman RM. Efflux of dopamine from the synaptic cleft in the nucleus accumbens of the rat brain. J Neurosci. 1994; 14:6084–6093. [PubMed: 7931564]

Garris, PA.; Wightman, RM. Regional differences in dopamine release, uptake, and diffusion measured by fast-scan cyclic voltammetry. In: AB; GB; RNA, editors. Neuromethods: Voltammetric Methods in Brain Systems. Humana Press Inc; 1995. p. 179-220.

Grace AA, Bunney BS. The control of firing pattern in nigral dopamine neurons: burst firing. J Neurosci. 1984; 4:2877–2890. [PubMed: 6150071]

Jacobs CB, Vickrey TL, Venton BJ. Functional groups modulate the sensitivity and electron transfer kinetics of neurochemicals at carbon nanotube modified microelectrodes. Analyst. 2011; 136:3557–3565. [PubMed: 21373669]

Jones SR, Garris PA, Kilts CD, Wightman RM. Comparison of dopamine uptake in the basolateral amygdaloid nucleus, caudate-putamen, and nucleus accumbens of the rat. J Neurochem. 1995; 64:2581–2589. [PubMed: 7760038]

Klapoetke NC, et al. Independent optical excitation of distinct neural populations. Nat Methods. 2014; 11:338–346. [PubMed: 24509633]

Lin JY, Knutsen PM, Muller A, Kleinfeld D, Tsien RY. ReaChR: a red-shifted variant of channelrhodopsin enables deep transcranial optogenetic excitation. Nat Neurosci. 2013; 16:1499–1508. [PubMed: 23995068]

Makos MA, Han K-A, Heien ML, Ewing AG. Using in Vivo Electrochemistry to Study the Physiological Effects of Cocaine and Other Stimulants on the Drosophila melanogaster Dopamine Transporter. ACS Chem Neurosci. 2010; 1:74–83. [PubMed: 20352129]

Makos MA, Kim Y-C, Han K-A, Heien ML, Ewing AG. In vivo electrochemical measurements of exogenously applied dopamine in Drosophila melanogaster. Anal Chem. 2009; 81:1848–1854. [PubMed: 19192966]

Marella S, Mann K, Scott K. Dopaminergic Modulation of Sucrose Acceptance Behavior in Drosophila. Neuron. 2012; 73:941–950. [PubMed: 22405204]

Martin CA, Krantz DE. Drosophila melanogaster as a genetic model system to study neurotransmitter transporters. Neurochem Int. 2014; 73:71–88. [PubMed: 24704795]

Nagel G, Szellas T, Huhn W, Kateriya S, Adeishvili N, Berthold P, Ollig D, Hegemann P, Bamberg E. Channelrhodopsin-2, a directly light-gated cation-selective membrane channel. Proc Natl Acad Sci. 2003; 100:13940–13945. [PubMed: 14615590]

Pandey UB, Nichols CD. Human disease models in Drosophila melanogaster and the role of the fly in therapeutic drug discovery. Pharmacol Rev. 2011; 63:411–436. [PubMed: 21415126]

Pörzgen P, Park SK, Hirsh J, Sonders MS, Amara SG. The antidepressant-sensitive dopamine transporter in Drosophila melanogaster: a primordial carrier for catecholamines. Mol Pharmacol. 2001; 59:83–95. [PubMed: 11125028]

Sabeti J, Adams CE, Burmeister J, Gerhardt GA, Zahniser NR. Kinetic analysis of striatal clearance of exogenous dopamine recorded by chronoamperometry in freely-moving rats. J Neurosci Methods. 2002; 121:41–52. [PubMed: 12393160]

Selcho M, Pauls D, Han K-A, Stocker RF, Thum AS. The role of dopamine in Drosophila larval classical olfactory conditioning. PLoS One. 2009; 4:e5897. [PubMed: 19521527]

Sullivan D, Pinsonneault JK, Pappa C, Zhu H, Lemeshow S, Mash DC, Sadee W. Dopamine transporter DAT and receptor DRD2 variants affect risk of lethal cocaine abuse: a gene-gene-environment interaction. Transl Psychiatry. 2013; 3:e222. [PubMed: 23340505]

Takmakov P, Zachek MK, Keithley RB, Bucher ES, McCarty GS, Wightman RM. Characterization of local pH changes in brain using fast-scan cyclic voltammetry with carbon microelectrodes. Anal Chem. 2010; 82:9892–9900. [PubMed: 21047096]

Taylor IM, Nesbitt KM, Walters SH, Varner EL, Shu Z, Bartlow KM, Jaquins-Gerstl AS, Michael AC. Kinetic diversity of dopamine transmission in the dorsal striatum. J Neurochem. 2015; 133:522–531. [PubMed: 25683259]

Vickrey TL, Condron B, Venton BJ. Detection of endogenous dopamine changes in Drosophila melanogaster using fast-scan cyclic voltammetry. Anal Chem. 2009; 81:9306–9313. [PubMed: 19842636]

Vickrey TL, Venton BJ. Drosophila Dopamine2-like receptors function as autoreceptors. ACS Chem Neurosci. 2011; 2:723–729. [PubMed: 22308204]

Vickrey TL, Xiao N, Venton BJ. Kinetics of the dopamine transporter in Drosophila larva. ACS Chem Neurosci. 2013; 4:832–837. [PubMed: 23600464]

Wightman RM, Zimmerman JB. Control of dopamine extracellular concentration in rat striatum by impulse flow and uptake. Brain Res Rev. 1990; 15:135–144. [PubMed: 2282449]

Wu Q, Reith MEA, Wightman RM, Kawagoe KT, Garris PA. Determination of release and uptake parameters from electrically evoked dopamine dynamics measured by real-time voltammetry. J Neurosci Methods. 2001; 112:119–133. [PubMed: 11716947]

Xiao N, Privman E, Venton BJ. Optogenetic control of serotonin and dopamine release in Drosophila larvae. ACS Chem Neurosci. 2014; 5:666–673. [PubMed: 24849718]

Yellman C, Tao H, He B, Hirsh J. Conserved and sexually dimorphic behavioral responses to biogenic amines in decapitated Drosophila. Proc Natl Acad Sci. 1997; 94:4131–4136. [PubMed: 9108117]

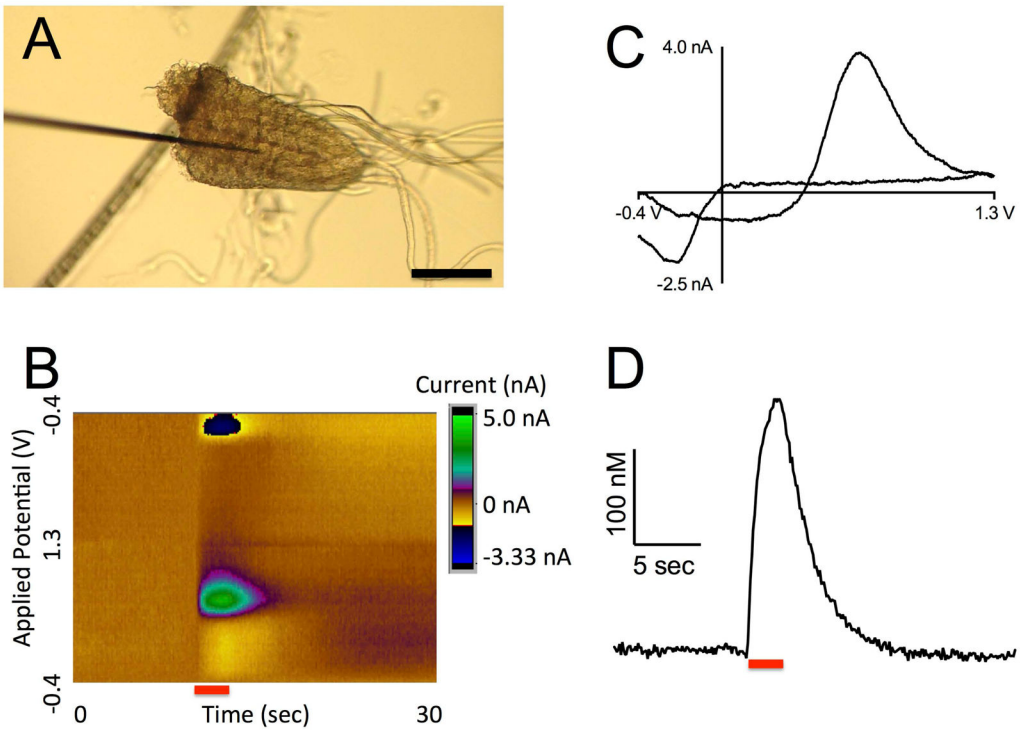

Figure 1. CsChrimson stimulated dopamine release from the ventral nerve cord of larval *Drosophila*

(A) A 7 μm carbon fiber microelectrode inserted into the neuropil of an isolated VNC through a cut surface. Scale bar is 50 μm. (B) False color plot of dopamine release in the VNC. The red bar marks the duration of a 2 s continuous light stimulation. Note the oxidation of dopamine in green and the reduction in dark blue during the stimulation. (C) Cyclic voltammagram of dopamine has characteristic oxidation (0.6 V) and reduction (−0.2 V) peaks for dopamine. This plot is a vertical cut through the color plot at time 12 sec. (D) Concentration of dopamine over time. Red light was applied for 2 seconds (red bar) causing a peak extracellular dopamine concentration of 262 nM. This plot is a horizontal cut through the color plot at 0.6 V, with current converted to concentration using a precalibration factor unique to the recording electrode (see *Electrochemical Measurements* in Materials and Methods).

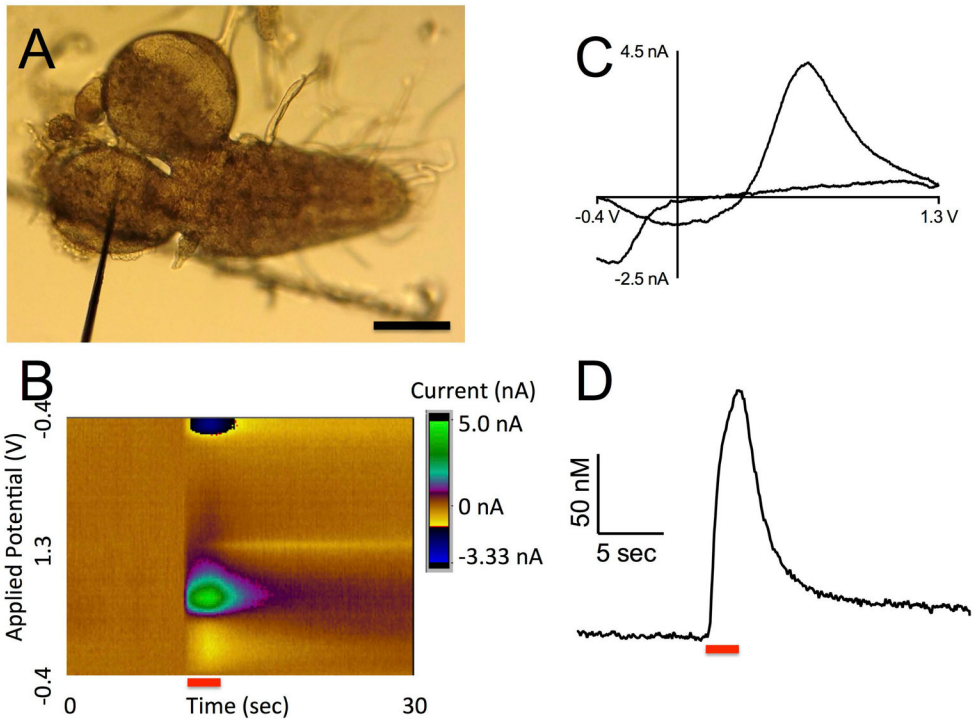

Figure 2. CsChrimson stimulated dopamine release from the protocerebrum of larval *Drosophila*

(A) A 7 μm carbon fiber microelectrode inserted into the medial protocerebrum through a lateral cut in the central nervous system. Scale bar is 50 μm. (B) False color plot of dopamine release in the protocerebrum. Note the oxidation of dopamine in green and the reduction in dark blue as the red light is applied to the sample (red bar). (C) Cyclic voltammagram of dopamine as it is oxidized (0.6 V) and reduced (−0.2 V). (D) Concentration of dopamine over time. Red light was applied for 2 seconds (red bar) causing a peak extracellular dopamine concentration of 155 nM.

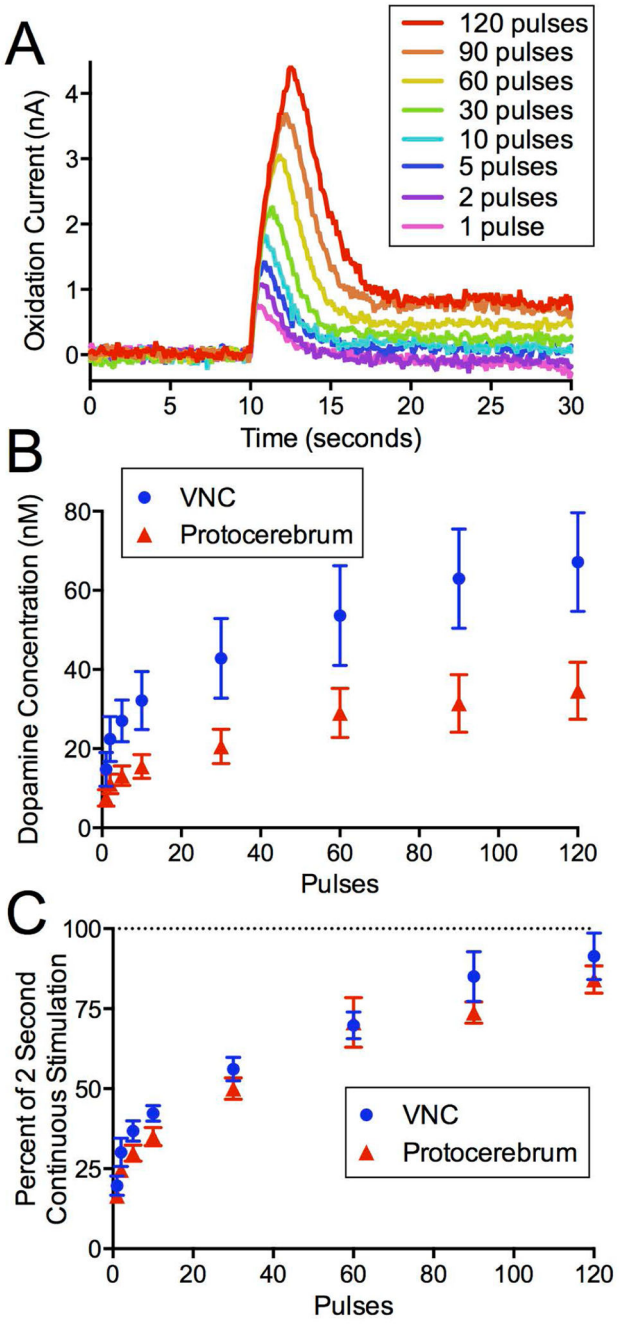

Figure 3. Extracellular dopamine increases similarly in the VNC and protocerebrum with red light exposure

(A) The peak oxidation current of dopamine over time as dopamine release is stimulated by increasing numbers of consecutive 4 ms red light pulses at 60 Hz in the VNC. (B) The amount of extracellular dopamine increases with number of pulses in both the VNC (blue circles, n=5) and the protocerebrum (red triangles, n=7). (C) Data (mean +/− SEM) are normalized to a 2 s continuous light stimulation to account for variation between animals.

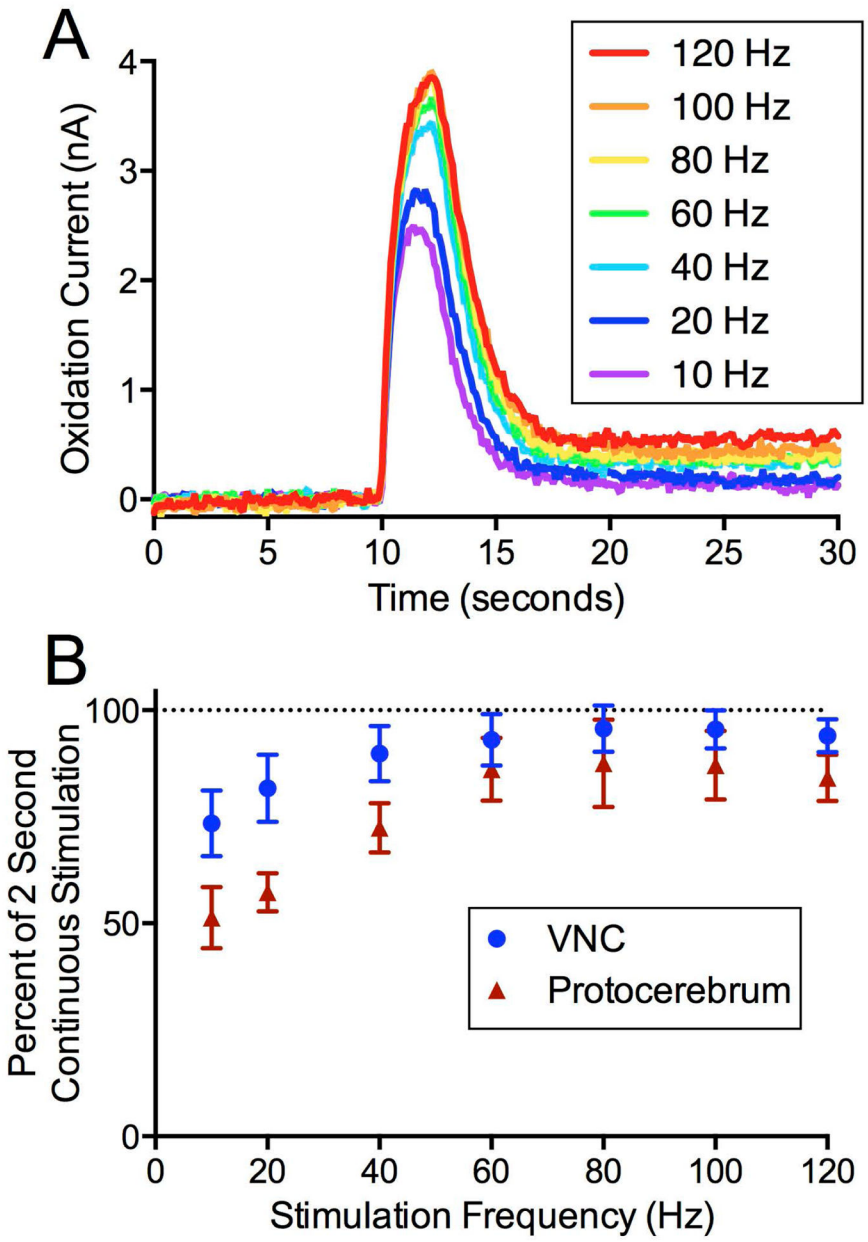

Figure 4. Extracellular dopamine increases with increasing light pulse frequency and then plateaus in both the VNC and protocerebrum

(A) The peak oxidation current of dopamine over time. Release is stimulated by different frequencies of 4 ms red light pulses for two seconds from the VNC. (B) The amount of extracellular dopamine detected in both the VNC (blue circles, n=7–9) and the protocerebrum (red triangles, n=5–7) increases with the frequency of red light pulses. Data (mean +/− SEM) are normalized to a 2 second continuous light stimulation to account for variation between animals.

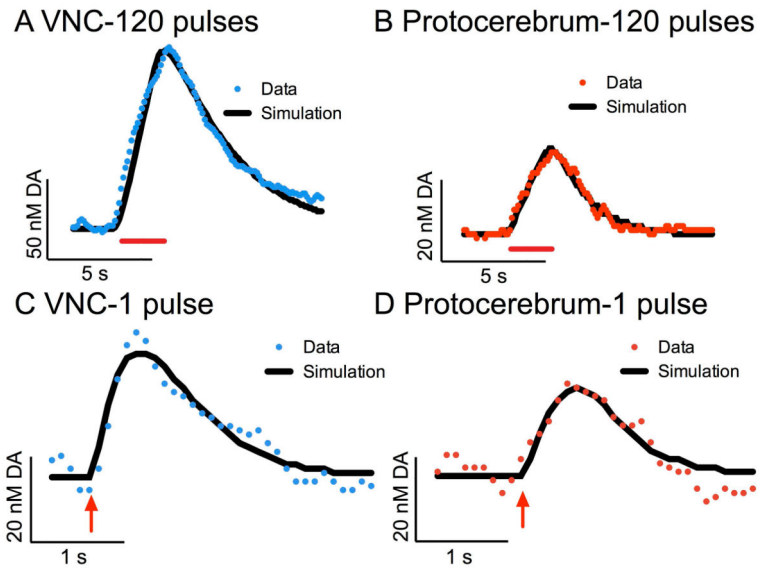

Figure 5. Michaelis-Menten modeling of dopamine release in the VNC and protocerebrum

Raw data (color dots) are plotted with the corresponding Michaelis-Menten model of the data (black line). (A) An example trace from the VNC (blue), which was stimulated with 4 ms red light pulses at 60 Hz for 2 seconds (red bar). The $[DA]_p$ is 1.0 nM, V_{max} is 0.03 μM/s, and K_m is 0.07 μM. R^2 for fit is 0.98. (B) An example trace from the protocerebrum (red), which was stimulated with 4 ms red light pulses at 60 Hz for 2 seconds (red bar). The $[DA]_p$ is 0.3 nM, V_{max} is 0.09 μM/s, and K_m is 0.14 μM. R^2 for fit is 0.97. (C) An example trace from the VNC (blue), which was stimulated with a single 4 ms red light pulse (red arrow). The $[DA]_p$ is 25 nM, V_{max} is 0.04 μM/s, and K_m is 0.09 μM. R^2 for fit is 0.91. (D) An example trace from the protocerebrum (red), which was stimulated with a single 4 ms red light pulse (red arrow). The $[DA]_p$ is 18 nM, V_{max} is 0.08 μM/s, and K_m is 0.10 μM. R^2 is 0.89.

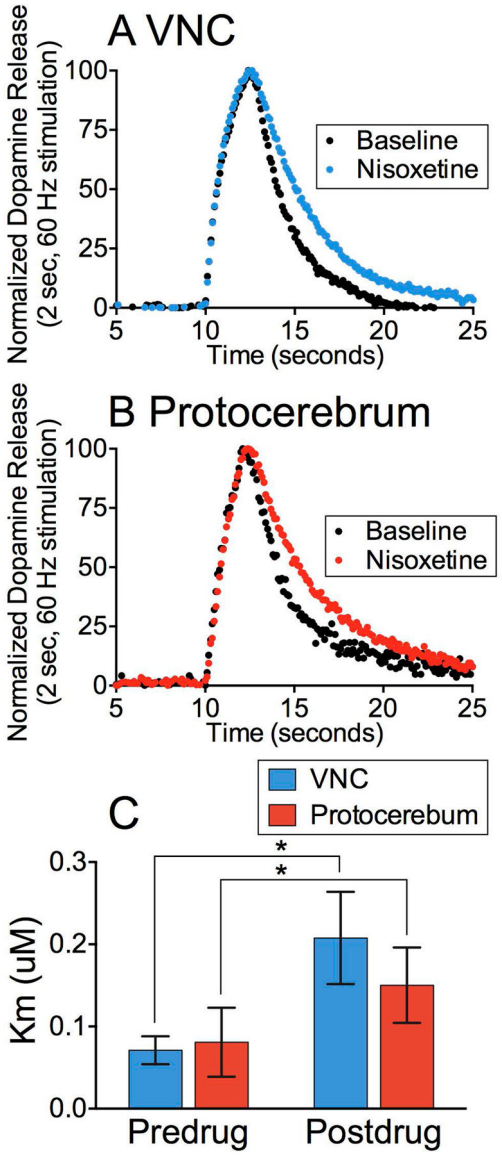

Figure 6. Nisoxetine acts as a competitive inhibitor, decreasing the affinity of dDAT for dopamine in both the VNC and protocerebrum

(A,B) A pulsed stimulation (2 sec, 60 Hz, 4 ms pulses; black) was taken in each animal and then repeated after 20 μM nisoxetine was applied for 20 minutes (color) in the (A) VNC and (B) Protocerebrum. The uptake rate decreased when the pre- and post-drug data are normalized for height and plotted together. (C) The kinetics were modeled for pre- and post-nisoxetine traces for the VNC (n=8) and Protocerebrum (n=6). There was a significant main effect of drug on the K_m (two-way ANOVA; p=0.0310, n=5–8), but not on V_{max} and $[DA]_p$ (two-way ANOVA; p>0.05, n=5–8, not shown). Data are mean +/− SEM.

Table 1
Kinetic values determined from Michaelis-Menten modeling

The dopamine released per pulse of red light ($[DA]_p$), V_{max}, and K_m of the VNC and protocerebrum with 1 (4 ms) pulse or 2 s stimulation (120 pulses, 4 ms, 60 Hz).

	$[DA]_p$ (nM)	V_{max} (μM/s)	K_m (μM)
Ventral nerve cord (1 pulse, n=4)	28 ± 12	0.04 ± 0.01	0.06 ± 0.02
Protocerebrum (1 pulse, n=5)	17 ± 3	0.11 ± 0.02	0.06 ± 0.01
Ventral Nerve Cord (120 pulses, 60 Hz, n=19)	0.93 ± 0.01	0.05 ± 0.01	0.10 ± 0.01
Protocerebrum (120 pulses, 60 Hz, n=9)	0.48 ± 0.01	0.08 ± 0.02	0.11 ± 0.02